A Lead-Dependent DNAzyme with a Two-Step Mechanism†

Andrea K. Brown, Jing Li, Caroline M.-B. Pavot, and Yi Lu*

Department of Chemistry, University of Illinois at Urbana-Champaign, Urbana, Illinois 61801

Received December 9, 2002; Revised Manuscript Received April 14, 2003

ABSTRACT: A detailed biochemical and mechanistic study of in vitro selected variants of 8−17 DNAzymes is presented. Even though the 8−17 DNAzyme motif has been obtained through in vitro selection under three different conditions involving 10 mM Mg^{2+} (called 8−17), 0.5 mM Mg^{2+}/50 mM histidine (called Mg5), or 100 μM Zn^{2+} (called 17E), all variants are shown to be the most active with Pb^{2+} (8−17: k_{obs} ~0.5 min^{-1}; Mg5: k_{obs} ~2 min^{-1}; 17E: k_{obs} ~1 min^{-1} with 200 μM Pb^{2+} at pH 5.0). For the 17E variant of the 8−17 DNAzyme, the single-turnover rate constants followed the order of $Pb^{2+} \gg Zn^{2+} \gg Mn^{2+} \approx Co^{2+} > Ni^{2+} > Mg^{2+} \approx Ca^{2+} > Sr^{2+} \approx Ba^{2+}$. The catalytic rate is half-maximal at 13.5 μM Pb^{2+}, 0.97 mM Zn^{2+}, or 10.5 mM Mg^{2+}, suggesting that the metal-binding affinity of the DNAzymes is in the order of $Pb^{2+} > Zn^{2+} > Mg^{2+}$. The Pb^{2+}-dependent activity increases linearly with pH and the slope of the plot of log k_{obs} versus pH is ~1, suggesting a single deprotonation in the rate-limiting step of the reaction. Sequence variations of the DNAzyme confirm the importance of the G•T wobble pair, the two loops and the intervening stem in maintaining the active conformation of the system. While Mg^{2+} and Zn^{2+} catalyze only a transesterification reaction with formation of a product containing a 2′,3′-cyclic phosphate, Pb^{2+} catalyzes a transesterification reaction followed by hydrolysis of the 2′,3′-cyclic phosphate. Although this two-step mechanism has shown to be operative in protein ribonucleases and in the leadzyme RNAzyme, it is now demonstrated for the first time that this DNAzyme may also use the same mechanism. Therefore, the two-step mechanism is observed in metalloenzymes of all classes, and this 8−17 DNAzyme provides a simple, stable, and cost-effective model system for understanding the structure of Pb^{2+}-binding sites and their roles in the two-step mechanism.

Lead-dependent, site-specific cleavage of RNA has been the focus of many research endeavors (*1*, *2*). The research may lead to a better understanding of lead toxicity in biological systems and provide a model system for studying the role of metal ions in DNA/RNAzymes (also called catalytic DNA/RNA or (deoxy)ribozymes) (*1*−*4*). The recent demonstration of a lead-dependent DNAzyme as a highly sensitive and selective lead biosensor (*5*) may stimulate further study in this field, as insight gained from the structure and mechanism of the DNAzyme may allow better design of metal biosensors (*6*).

Lead is known to efficiently depolymerize RNA, which may be responsible for lead toxicity in biology. The discovery by Werner et al. (*7*) that Pb^{2+} promotes site-specific cleavage of yeast transfer RNA^{phe} prompted detailed X-ray crystallographic studies by Klug and co-workers (*3*, *8*). The studies on the cleaved (at pH 7.4) and uncleaved (at pH 5.0) $tRNA^{Phe}$−lead complexes revealed a lead ion, termed Pb(1), being responsible for the cleavage between residues U17 and G18. With a pK_a of 7.8, the lead hydrate exists in a partially deprotonated form at pH 7.4. Pb(1) was located ~6.0 Å from the oxygen atom of the 2′-OH of ribose 17 and precisely coordinated in a pocket formed by eight residues in the D and T loops in such a way that it could remove the proton from the 2′-hydroxyl of ribose 17 (*12*). The authors proposed that the resulting 2′-O^- nucleophile could then attack phosphate 17 to give a pentacoordinated phosphorus intermediate, which decayed to form the 2′,3′-cyclic phosphate and 5′-OH termini (*7*). This mechanism has been extended to explain RNA cleavage induced by other metal ions.

The above work on the study of $tRNA^{Phe}$−lead complexes motivated Pan and Uhlenbeck to develop an in vitro selection method to isolate, from a randomized $tRNA^{Phe}$, small (22−30-mer) lead-dependent RNAzymes or ribozymes (termed leadzymes) (*4*, *9*). They demonstrated that the leadzymes not only catalyze site-specific RNA cleavage to form 2′,3′-cyclic phosphate and 5′-OH termini but also promote hydrolysis of the 2′,3′-cyclic phosphate to produce specifically 3′-monophosphate. This two-step (cleavage followed by hydrolysis) mechanism, although common in protein ribonucleases, appears to be unique among nucleic acid enzymes (*4*). Therefore, many biochemical (*10*−*17*), NMR (*18*−*21*), and X-ray crystallographic (*22*) studies have been reported to provide insight into the structure and function of this model metallo−RNAzyme. For example, it was discovered that the reaction of the leadzyme is enhanced by the combined effect of lead and rare earth ions (*11*, *12*). NMR studies have found unusual dynamics and pK_a shifts of bases at the active site of the leadzyme (*18*−*21*). Finally, crystallographic study revealed a metal ion in close proximity to the 2′-OH of the cleavage ribose (*22*).

† This material is based upon work supported by the Natural and Accelerated Bioremediation Research (NABIR) program, Biological and Environmental Research (BER), U.S. Department of Energy (DEFG02-01-ER63179). Y.L. is a Cottrell Scholar of the Research Corporation and a Camille Dreyfus Teacher-Scholar of the Camille and Henry Dreyfus Foundation.

* To whom correspondence should be addressed. Tel: (217) 333-2619. Fax: (217) 333-2685. E-mail: yi-lu@uiuc.edu.

10.1021/bi027332w CCC: $25.00
Published on Web 05/23/2003

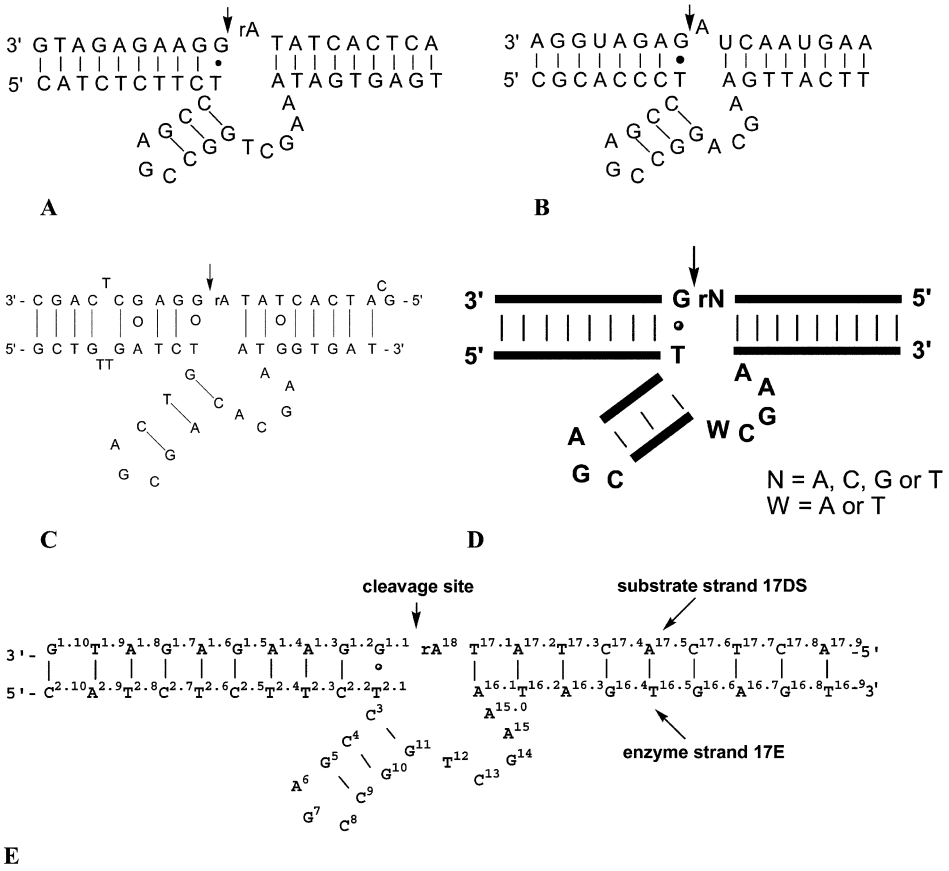

FIGURE 1: (A−C) Sequences of the 17E (A), 8−17 (B), and Mg5 (C) DNAzymes. The arrow indicates the cleavage site. (D) Conserved sequence and proposed secondary structure (*26*) of the trans-cleaving 8−17 DNAzyme. The thick lines represent the nucleotides on the helical regions. The thin lines represent the Watson−Crick base pairs across the helices. (E) The nucleotides of 17E are numbered by a system analogous to that used for the hammerhead ribozyme (*45*) and proposed by Peracchi (*27*).

Compared with what is known about the lead−tRNA and lead−RNAzymes, much less information about lead-dependent DNAzymes has been reported. This is despite the fact that the first DNAzyme reported in the literature is a lead-dependent DNAzyme (*23*), which was studied by Geyer and Sen using lanthanide ions as probes (*24*). A detailed study of the properties and mechanism of a lead-dependent DNAzyme is highly desirable for several reasons. First, it will provide an alternative model system that is less expensive to synthesize and more stable than the lead−RNAzyme system. Second, comparing and contrasting lead−tRNA, lead−RNAzyme, and lead−DNAzyme systems may allow a comprehensive understanding of lead−nucleic acid interactions. For example, it would be quite interesting to find out if the lead ion in DNAzymes promotes the single-step mechanism, as in $tRNA^{Phe}$, or the two-step mechanism, as in the leadzyme. Finally, it may provide insight for designing better lead sensors.

We are interested in the study of the lead-dependent cleavage properties and mechanism of 8−17 DNAzymes (Figure 1). They were isolated by three groups using three different conditions (Table 1). The 17E DNAzyme was selected in solution containing Zn^{2+} (*25*). The conserved region of its structural motif (Figure 1A) was found (*25*) to be very similar to that of the 8−17 DNAzyme selected by Santoro and Joyce using Mg^{2+} as a cofactor (Figure 1B) (*26*). Interestingly, a similar sequence motif was also observed (*27*) in an RNA-cleaving DNAzyme called Mg5 selected by Faulhammer and Famulok using 50 mM histidine and 0.5 mM Mg^{2+} as cofactors (Figure 1C) (*28*, *29*).

Table 1: Comparison of the Random Pool and Selection Conditions of the in Vitro Selection Experiments for 17E, 8−17, and the Mg5 DNAzymes

	17E	8−17	Mg5
	Random pool		
length	106	99	141
no. of random-bases	40	50	74
no. of RNA bases	1	12	1
	Selection conditions		
cofactor	100 μM Zn^{2+}	10 mM Mg^{2+}	50 mM histidine 0.5 mM Mg^{2+}
buffer	50 mM HEPES	50 mM Tris-HCl	50 mM sodium-phosphate
pH	7.0	7.5	7.0
salt	500 mM NaCl	1 M NaCl	125 mM NaCl 125 mM KCl
temperature (°C)	25	37	37
references	*25*	*26*	*28*, *29*

The conserved region of the 8−17 DNAzymes has been defined by Santoro and Joyce (Figure 1D) (*26*). The unpaired bulge region in the 8−17 DNA enzyme has the sequence 5′-WCGR-3′ or 5′-WCGAA-3′ (W = A or T; R = A or G). Among the Zn(II)-dependent 17E DNAzymes we obtained after reselection (*25*), 85% of them fell within the 5′-WCGAA-3′ regime (W = A or T). However, the sequence of the two double helices flanking the catalytic core is different between the 8−17 and the 17E DNAzymes,

reflecting their different designs of the selection pool. For Mg5 DNAzymes, the homologous region in 31 out of the 44 sequenced clones had the sequence 5′-$TX_1X_2X_3AGCY_1Y_2Y_3ACGAA$-3′, falling within the WCGAA-3′ regime. The authors predicted a secondary structure different from the 8−17 or 17E motif based on chemical modification analysis. However, a structure containing a three-way junction similar to that of the 17E and 8−17 DNAzymes is consistent with the chemical mapping results. Experimental support for the similarity between 8−17 and Mg5 DNAzymes has been provided by Peracchi (*27*).

Initial biochemical assays indicated that Mg5 is active in Mg^{2+}, Mn^{2+}, Ca^{2+}, or Zn^{2+} with metal-dependent activity in the order of $Zn^{2+} \gg Ca^{2+} > Mg^{2+}$ under similar conditions (*25*−*29*). However, further tests from our research group showed that the 17E variant of the 8−17 DNAzyme is much more active in the presence of Pb^{2+} than any other metal ions tested. Therefore, it was made into a lead biosensor by attaching a fluorophore and a quencher to the 5′-end of the substrate and 3′-end of the enzyme, respectively (*5*).

Here, we report for the first time a detailed biochemical study of the lead-dependent properties of all three variants of the DNAzyme and show that they are the most active with Pb^{2+}. More importantly, we show that the 17E DNAzyme shares the same two-step mechanism with protein enzymes such as ribonucleases and RNAzymes such as the leadzyme, thus demonstrating that the two-step mechanism is no longer unique to proteins and RNAzymes.

MATERIALS AND METHODS

Preparation of Oligonucleotides and Other Reagents. Oligonucleotides were purchased from Integrated DNA Technologies, Inc. and purified by reverse-phase HPLC. Ultrapure lead acetate from Sigma was used without purification. To make the MES buffer (2-[*N*-morpholino]-ethane sulfonic acid), 500 mM solutions of ultrapure MES monohydrate and MES sodium salt (from Sigma) were made with deionized water (through a Millipore Milli-Q Synthesis system). The solutions were treated overnight with Chelex beads (iminodiacetic acid, from Sigma) to remove any divalent metal ions present. The solutions were then mixed to obtain the proper pH, and the resulting buffer was then filtered with a 0.2-micron syringe filter and stored in microcentrifuge tubes at −20 °C. The microcentrifuge tubes had been pretreated with 10% HNO_3, rinsed with deionized water, and dried to remove any divalent metal ions present on the surface. The sodium acetate buffer was made in a similar fashion, using ultrapure sodium acetate and acetic acid (from Fisher).

Kinetic Assays. The 17DS substrate was 5′-labeled with $^{\gamma}AT^{32}P$ (from Amersham) using T4 kinase from Invitrogen. The enzyme and substrate were annealed in a 95 °C water bath for 2 min and were then placed in a block heater set at 28 °C for 15 min in order to equilibrate to that temperature. The tubes were then kept in the block heater for the duration of the assay to prevent temperature fluctuations.

The assays were conducted under single-turnover conditions. The final concentrations of the enzyme and substrate were 5 μM and 0.5 nM, respectively, for all assays, unless indicated otherwise. The final concentration of buffer was 50 mM. If sodium nitrate was added to the reaction, the final concentration was 100 mM. After annealing the solution of enzyme and substrate and allowing solutions to equilibrate to 28 °C, an aliquot of the solution was taken out and added to 5 μL of stop solution (50 mM EDTA, 8 M urea, 90 mM Tris, 90 mM boric acid, 0.05% xylene cyanol, and 0.05% bromophenol blue) as a control to indicate the extent of cleavage before the reaction was initiated. The reaction was initiated by addition of an equal volume of a solution of Pb^{2+} acetate to the enzyme/substrate solution. Unless stated otherwise, the final concentration of Pb^{2+} in the reaction mixture was 200 μM. At various predetermined time-points, a 2 μL aliquot of the reaction mixture was added to 5 μL of stop solution in a 96-well plate.

The uncleaved substrate and cleaved products were separated by 20% denaturing polyacrylamide gel electrophoresis and quantified by a Molecular Dynamics Storm 430 phosphorimager (from Amersham Biosciences). The percent product at time t, $\%P_t$, was calculated by dividing the amount of 5′-cleavage product by the total amount of substrate plus product, after subtraction of background radioactivity in the gel. Kinetic curves were plotted using SigmaPlot and fit to the equation

$$\%P_t = \%P_0 + \%P_\infty(1 - e^{-kt})$$

where $\%P_0$ is the initial percent product (at $t = 0$), $\%P_\infty$ is the percent product at the endpoint of the reaction ($t = \infty$), and k is the rate of cleavage (*30*).

The enzyme-dependent activities were analyzed by plotting k_{obs} (in min^{-1}) versus enzyme concentration in μM and fitting the resulting curve to the equation

$$k_{obs} = \frac{k_{cat}[E]}{K'_M + [E]}$$

where k_{cat} is the second-order rate constant, and k_{obs} is the pseudo-first-order rate constant under steady-state conditions. K'_M is the Michaelis−Menten constant determined at single-turnover conditions.

For the pH-dependent enzyme activity study, $\log(k_{obs})$ was plotted as a function of pH. The curve was fit to a straight line. For the lead-dependence curve, k_{obs} was plotted as a function of Pb^{2+} concentration. The curve was fit to the equation

$$k_{obs} = \frac{k_{max}[M^{2+}]}{K_{d,app} + [M^{2+}]}$$

where k_{max} is the maximum observed rate constant at the point of saturation of Pb^{2+} concentration, and $K_{d,app}$ is the apparent binding constant of Pb^{2+} to the enzyme/substrate complex.

The rate of reaction was also determined for alternative sequences of the enzyme and substrate. In each case, the final concentrations were 5 μM enzyme, 0.5 nM substrate, 50 mM sodium acetate (pH 5.0), 200 μM Pb^{2+}, and 100 mM sodium nitrate, and the experiments were conducted at 28 °C. For the reaction mixtures containing Zn^{2+}, the concentrations were 5 μM enzyme, 0.5 nM substrate, 50 mM MES (pH 6.0), and 5 mM Zn^{2+}. The rate constants listed are an average of at least two independent experiments.

Products Analysis by MALDI-MS. The products obtained by the 17E reaction in the presence of Pb^{2+}, Zn^{2+}, and Mg^{2+} were analyzed by mass spectrometry. Each reaction mixture contained 2.5 μM 17DS, 2.5 μM 17E, and 50 mM HEPES (pH 7.4). After annealing the enzyme and substrate and allowing them to cool, the reactions were initiated by addition of 500 μM Zn^{2+}, 50 μM Pb^{2+}, or 2 mM Mg^{2+} and were allowed to proceed at 28 °C. The reactions were stopped by addition of EDTA for a final concentration of 10 mM (25 mM for Mg^{2+}). The product mixtures were then desalted on Sep-Pak C-18 columns (from Waters) and lyophilized.

For MALDI-MS analysis, the samples were dissolved in 0.1 M triethylammonium acetate, pH 7.0, and desalted with $ZipTip_{C18}$ pipet tips (from Millipore) before analysis by mass spectrometry. The sample was diluted in the matrix to a concentration of 2−10 μM, and the matrix consisted of a mixture of 2′,4′,6′-trihydroxyacetophenone monohydrate and ammonium citrate. The Voyager DE-STR MALDI-TOF spectrometer (from Applied Biosystems) was calibrated using angiotensin (MW 1296.7 g/mol) and insulin (MW 5734.5 g/mol). Data were taken in the linear-extraction, positive ion mode, with an acceleration voltage of 20 000 V and a delay of 150 ns.

The mechanism of cleavage of 17E in the presence of Pb^{2+} was investigated by analysis of the hydrolysis of cP_1 with the enzyme/product 2 complex, $17EP_2$ (Figure 6), present in the mixture. The reaction mixtures contained 5 μM $17EP_2$, 2.5 μM cP_1, 200 μM Pb^{2+}, and 50 mM HEPES (pH 7.4). Controls contained cP_1 alone, cP_1 with 17EP2, and cP_1 with Pb^{2+}. $17EP_2$ and cP_1 were annealed at 95 °C for 2 min and cooled at 28 °C for 15 min. The reaction was initiated by addition of Pb^{2+} and was allowed to proceed at 28 °C for various times from 2 min to 3 h. The reactions were stopped by addition of EDTA for a final concentration of 10 mM, and the volume was concentrated to approximately 10 μL. The sample composition was then analyzed by MALDI-TOF mass spectrometry.

The rate of hydrolysis was measured by 5′ ^{32}P-labeling the purified cP_1 product (see below). A large excess of unlabeled cP_1 (2.5 μM vs 0.5 nM labeled cP_1) in HEPES buffer (pH 7.4) was added to a solution containing either 200 μM Pb^{2+} or 10 mM Mg^{2+}, with and without the $17EP_2$ complex added. Aliquots of the reaction mixture were taken out at various times and added to a stop solution containing 9 M urea and 50 mM EDTA. The aliquots were then analyzed on a 25% denaturing polyacrylamide gel and quantified using a phosphorimager.

Isolation of the Cyclic Phosphate Product (cP_1). 17DS was cleaved in the presence of magnesium to obtain the cyclic phosphate product, cP_1 (2′,3′-cyclic phosphate, a 10-mer) and the product P_2 (also a 10-mer). cP_1 traveled faster on the gel than P_2, which could be due to differences in charge or polarity of the two products. Therefore, the products were separated by high-resolution polyacrylamide gel electrophoresis. The reaction mixture contained 2 nmol 17DS, 1 nmol 17E, 30 mM Mg^{2+}, and 50 mM HEPES (pH 7.4). The enzyme and substrate were heated for 2 min at 95 °C and then cooled at room temperature for 15 min. The reaction was initiated by addition of the metal ion and was allowed to proceed at 28 °C for approximately 8 h. The reaction was stopped by addition of a 3-fold excess of EDTA over Mg^{2+}. The product mixture was then desalted on a Sep-Pak C-18 column, lyophilized, and dissolved in loading buffer (10 mM EDTA, 90% formamide). The products were separated by 20% denaturing polyacrylamide gel electrophoresis. The band of interest was detected using UV-shadowing, cut out, crushed, and soaked in a solution of 10 mM Tris buffer and 1 mM EDTA, pH 7.5. After three buffer changes, at 2, 4, and 12 h, the samples were pooled and desalted using a Sep-Pak C-18 column. The purified cP_1 was then lyophilized and dissolved in autoclaved deionized water. The concentration was determined by measuring the absorbance at 260 nm on a Hewlett-Packard 8453 UV/vis spectrometer and using $\epsilon = 100\,700\ M^{-1}\ cm^{-1}$, as calculated using the Biopolymer Calculator (http://paris.chem.yale.edu/extinct.html).

Table 2: Rate Constants of the 17E DNAzyme in the Presence of Selected Divalent Metal Ions at pH 6.0

metal ion	k_{obs} (min^{-1})[a]	pK_a[b]
Ba^{2+}	0.0003	13.82
Sr^{2+}	0.0005	13.18
Mg^{2+}	0.017	11.42
Ca^{2+}	0.015	12.7
Ni^{2+}	0.008	9.86
Co^{2+}	0.25	9.65
Mn^{2+}	0.24	10.6
Zn^{2+}	1.35	8.96
Pb^{2+}	5.75	7.8

[a] The concentration of metal ions used in the study is 10 mM, except that the Pb^{2+} concentration is 100 μM. [b] The pK_a value of each hydrated metal ion (*44*) is listed for comparison.

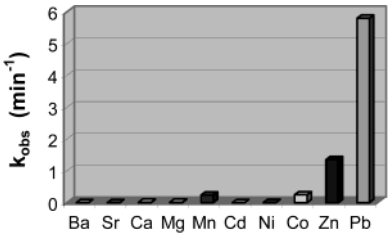

FIGURE 2: Single turnover rate constants of the 17E DNAzyme in the presence of different divalent metal ions at pH 6.0. All metal ion concentrations are 10 mM, except for Pb^{2+}, which is 100 μM.

RESULTS

Dependence of Activity on Divalent Metal Ions and pH. Kinetic assays of the 17E variant of 8−17 DNAzyme (Figure 1A) in the presence of different metal ions were carried out at pH 6.0. This pH was chosen because the high Pb^{2+}-dependent activity at physiological pH (7.5) precluded accurate determination of the single-turnover rate constants using the common assay method of initiating and terminating the reactions with manual pipet mixing. The concentration of Pb^{2+} was 0.1 mM, as opposed to 10 mM for all other metal ions, for the same reason. The results are summarized in Table 2 and displayed in Figure 2. The single-turnover rate constants followed the order of $Pb^{2+} \gg Zn^{2+} \gg Mn^{2+} \approx Co^{2+} > Ni^{2+} > Mg^{2+} \approx Ca^{2+} > Sr^{2+} \approx Ba^{2+}$.

To determine if all three variants (17E, 8−17, and Mg5) of the DNAzyme are the most active in Pb^{2+}, we investigated the Zn^{2+}- and Pb^{2+}-dependent activity of the 8−17 (Figure 1B) and Mg5 (Figure 1C) variants. In the presence of 200 μM Pb^{2+} (pH 5.0) and 5 mM Zn^{2+} (pH 6.0), the 17E variant has a k_{obs} of 0.99 and 0.99 min^{-1}, respectively. Under the

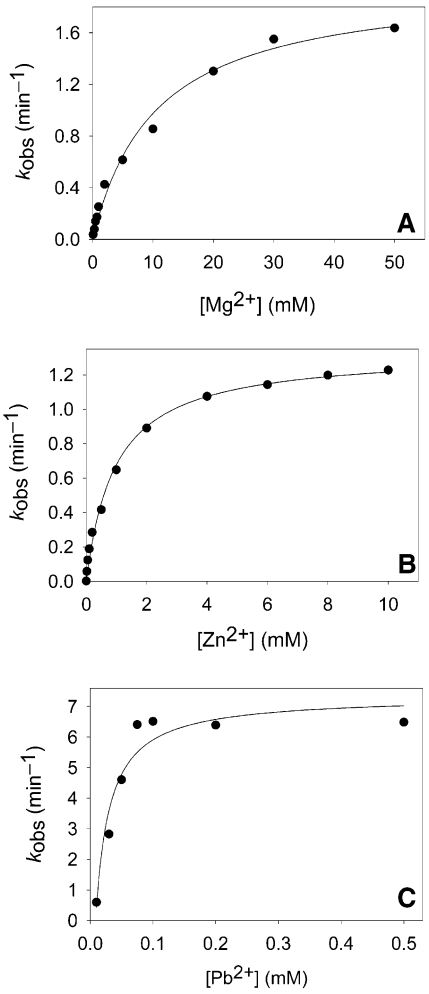

FIGURE 3: Dependence of the single-turnover rate constants on the concentration of divalent metal ion. Reactions were carried out in the presence of either (A) Mg^{2+} (at pH 7.0), (B) Zn^{2+} (at pH 6.0), or (C) Pb^{2+} (at pH 6.0).

same conditions, the k_{obs} for 8−17 was found to be 0.47 and 0.12 min^{-1} with Pb^{2+} (at pH 5.0) and Zn^{2+} (at pH 6.0), respectively. For Mg5, k_{obs} was found to be 2.1 and 0.74 min^{-1} with Pb^{2+} (at pH 5.0) and Zn^{2+} (at pH 6.0), respectively. Because of the similar behavior of all three variants of the 8−17 DNAzymes, the work presented here focuses mainly on the 17E variant.

To define more completely the metal ion-dependent activity of 17E, we investigated the dependence of cleavage rate on the concentration of Mg^{2+}, Zn^{2+}, and Pb^{2+}. More than 95% of the substrate could be cleaved in all three metal ions, suggesting that the majority of the enzyme was active in these three metal ions. At pH 7.0, the cleavage rates in the presence of high concentrations of Pb^{2+} and Zn^{2+} are too fast for accurate determination using the conventional assay method described above. To obtain rate constants over a broad range of both unsaturating and saturating metal concentrations, the cleavage reactions in the presence of Zn^{2+} and Pb^{2+} were performed at pH 6.0, where the cleavage rate should be 10-fold slower (on the basis of the pH-dependent rate profile presented in the next section). The reaction in Mg^{2+} was performed at pH 7.0 since the rate in low concentrations of Mg^{2+} was too slow to measure at pH 6.0. The catalytic rate was half-maximal at 13.5 ± 6.0 μM Pb^{2+}, 0.997 ± 0.085 mM Zn^{2+}, or 10.5 ± 1.6 mM Mg^{2+} (Figure 3), suggesting that the metal-binding affinity of the DNAzymes is in the order of Pb^{2+} > Zn^{2+} > Mg^{2+}.

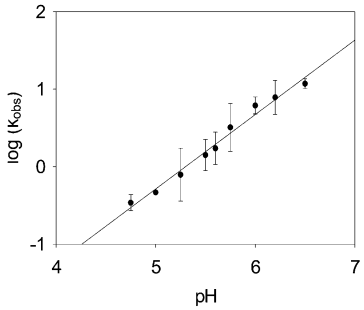

FIGURE 4: Dependence of the rate of substrate cleavage on the pH. The curve was plotted, with error bars, from an average of three separate experiments. The reactions were all carried out at 28 °C with 5 μM 17E, 0.5 nM 17DS, 50 mM NaOAc (pH 5.0), 200 μM Pb^{2+}, and 100 mM $NaNO_3$. The slope of the line is equal to ~1, with an R^2 value of 0.983.

To help extrapolate the high rate constants at physiological pH and to provide insight into the reaction mechanism, the lead-dependent DNAzyme activity was assayed under different pH values. Figure 4 displays the log(k_{obs}) as a function of pH for assays performed at 28 °C with 5 μM enzyme, 0.5 nM substrate, 200 μM Pb^{2+}, 100 mM sodium nitrate, and 50 mM sodium acetate at different pH values. The slope of the line is approximately equal to 1, suggesting a single deprotonation in the rate-limiting step of the reaction, which is similar to the findings for the hammerhead ribozyme (*31*), the leadzyme (*10*), and other DNAzymes (*25*, *32*).

Dependence of Activity on Sequence Variations. Figure 5 shows a plot of the observed single turnover rate constants versus enzyme concentration in the range of 100 nM to 10 μM 17E at pH 5.0. From this curve, the K'_M and k_{cat} were calculated to be 0.52 ± 0.12 μM and 0.50 ± 0.03 min^{-1}, respectively, for the wild-type 17E DNAzyme (Figure 1A) at this pH.

Since the G•T wobble pair is conserved in the DNAzyme, effects of its variation on the activity were investigated. The rate constants were measured for several sequence variations. These are summarized in Table 3. The nucleotides were numbered as shown in Figure 1E. When the G•T wobble pair was reversed as in (E) $T^{2.1}$ → G/(S) $G^{1.1}$ → T, catalysis was completely inhibited, with no cleavage after 24 h. Catalysis was also abolished when the G•T wobble pair was replaced by a G−C base pair, (E) $T^{2.1}$ → C. Furthermore, one class in the original selection pool contains another G•T wobble pair next to the above G•T wobble pair (*25*, *33*). Introduction of this second G•T wobble pair back into the DNAzyme, (E) $C^{2.2}$ → T, caused a ~10-fold decrease of reaction rate in the presence of both Pb^{2+} (0.10 min^{-1}) and Zn^{2+} (0.091 min^{-1}). However, introduction of a second G•T wobble pair on the 5′ side of the cleavage site of the substrate, (E) $A^{16.1}$ → G, resulted in only a 2- and 3-fold decrease in reaction rate with Pb^{2+} (0.40 min^{-1}) and Zn^{2+} (0.30 min^{-1}), respectively.

Additional variations in the 17E sequence were also investigated. The mutant (E) − $A^{15.0}$; T^{12} → A, which contains the same catalytic core as the 8−17 DNAzyme (*26*), was found to have a rate of 0.47 min^{-1} with Pb^{2+} and 0.12 min^{-1} with Zn^{2+}. Another mutant, containing a catalytic core corresponding to that of the Mg5 DNAzyme (*28*, *29*), was

Table 3: Rate Constants for the 17E DNAzyme and Its Variants in the Presence of 200 μM Pb^{2+} (pH 5.0) and 5 mM Zn^{2+} (pH 6.0)[a]

8−17 Variant	200 μM Pb^{2+}		5 mM Zn^{2+}	
	k_{obs} (min^{-1})	relative rate	k_{obs} (min^{-1})	relative rate
17E	0.99	1.0	0.99	1.0
(E) − $A^{15.0}$; T^{12}→A(8−17)	0.47	0.47	0.12	0.12
(E) T^{12}→A; C^{3}→G; C^{4}→T; G^{5}→C; C^{9}→G; G^{10}→A; G^{11}→C (Mg5)	2.06	2.06	0.74	0.74
(E) $T^{2.1}$→G; (S) $G^{1.1}$→T	N.D.		N.D.	
(E) $T^{2.1}$→C	N.D.		N.D.	
(E) $C^{2.2}$→T	0.10	0.10	9.1×10^{-2}	9.1×10^{-2}
(E) $A^{16.1}$→G	0.40	0.41	0.30	0.30
(E) − $A^{15.0}$	0.38	0.39	0.36	0.36
(E) − T^{12}	4.8×10^{-3}	4.9×10^{-3}	2.6×10^{-3}	2.6×10^{-3}
(E) + $G^{4.0}$; + $C^{9.0}$	3.7×10^{-3}	3.8×10^{-3}	6.9×10^{-3}	6.9×10^{-3}
(E) C^{4}→A; G^{10}→T	0.43	0.43	0.18	0.18
(E) + $A^{6.0}$	2.1×10^{-2}	2.1×10^{-3}	2.9×10^{-2}	2.9×10^{-2}
(E) A^{6}→C; C^{8}→A	3.0×10^{-3}	3.0×10^{-3}	3.8×10^{-3}	3.8×10^{-3}
(E) − $T^{16.9}$	0.92	0.92	0.91	0.92
(E) − $T^{16.9}$, $G^{16.8}$	0.91	0.92	0.91	0.92

[a] The nucleotides are numbered as shown in Figure 1E. An (E) indicates a mutation in the enzyme strand, and an (S) indicates a mutation in the substrate. A (−) indicates the deletion of a nucleotide, and a (+) indicates the insertion of a nucleotide. For example, + $A^{6.0}$ indicates the insertion of an adenosine between A^6 and G^7. The letters N.D. indicate that the cleavage activity was not detectable after 24 h. The relative rate is the rate as compared to that of the original 17E sequence. The second and third entries are mutants containing a catalytic core corresponding to the 8−17 and Mg5 DNAzymes, respectively.

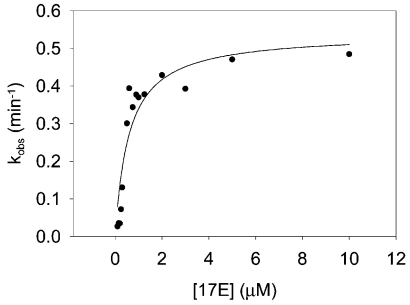

FIGURE 5: The enzyme dependence curve was obtained at a constant temperature of 28 °C with 0.5 nM 17DS (5′- ^{32}P labeled), 50 mM NaOAc (pH 5.0), 200 μM Pb^{2+}, and 100 mM $NaNO_3$.

shown to have a rate of 2.1 min^{-1} with Pb^{2+} and 0.74 min^{-1} with Zn^{2+}.

Removal of an adenosine from the 5-nucleotide loop, (E) − $A^{15.0}$, produced a 3-fold decrease in reaction rate (0.38 min^{-1} with Pb^{2+} and 0.36 min^{-1} with Zn^{2+}) as compared to the reaction with 17E under the same conditions (0.99 min^{-1} with both metals). However, removal of the thymidine from the same loop, (E) − T^{12}, decreased the rate by more than 2 orders of magnitude (0.0048 min^{-1} with Pb^{2+} and 0.0026 min^{-1} with Zn^{2+}). The reaction rate for (E) + $G^{4.0}$; + $C^{9.0}$, a 17E mutant containing a fourth G−C pair in the 3-base pair stem, was more than 2 orders of magnitude slower than the rate for 17E (0.0037 min^{-1} with Pb^{2+} and 0.0069 min^{-1} with Zn^{2+}). Substitution of an A−T base pair for the second G−C base pair in the stem, (E) C^4 → A; G^{10} → T, resulted in a 2- and 5-fold decrease in reaction rate with Pb^{2+} (0.43 min^{-1}) and Zn^{2+} (0.18 min^{-1}), respectively.

The 3-nucleotide loop seemed particularly susceptible to mutation, as a mutant containing an additional adenosine, (E) + $A^{6.0}$, and a mutant in which the sequence of the loop was reversed, (E) A^6 → C; C^8 → A, both caused a decrease in the reaction rate by around 2 orders of magnitude with Pb^{2+} (0.021 and 0.0030 min^{-1}, respectively) and Zn^{2+} (0.029 and 0.0038 min^{-1}, respectively). Interestingly, two truncated forms of the enzyme missing one or two nucleotides from the 3′ end, (E) − $T^{16.9}$ and (E) − $T^{16.9}$; $G^{16.8}$, showed very similar activity to 17E, indicating that reducing the number of base pairs between enzyme and substrate has little effect on the rate of the single-turnover reaction.

Table 4: Rate Constants of the 17E DNAzyme with Different RNA Bases at the Cleavage Site, rN^{18}, in the Presence of 200 μM Pb^{2+} or 500 μM Zn^{2+} Ions

reaction conditions	Identity of the RNA Base at the Cleavage Site			
	rA^{18}	rG^{18}	rC^{18}	rU^{18}
200 μM Pb^{2+}, NaOAc, pH 5.0 (min^{-1})	0.47	0.34	0.024	0.015
500 μM Zn^{2+}, MES, pH 6.0 (min^{-1})	0.49	0.57	0.066	0.029

In addition to the above experiments, the effect of RNA base identity at the cleavage position on the reaction rate was also studied. As shown in Table 4, the rate is approximately 10-fold faster for purine bases (G and A) than for pyrimidine bases (C and U) in the presence of Pb^{2+} or Zn^{2+}.

Reaction Products Analysis. The cleavage products of the DNAzyme were identified using MALDI-TOF mass spectrometry. The products were generated by reacting the substrate 17DS with 17E for 15 min in the presence of 2 mM Mg^{2+}, 500 μM Zn^{2+}, or 50 μM Pb^{2+} in HEPES buffer (pH 7.4). For all three metal ions, two major signals were identified for the cleavage products of 17DS with the mass of 3050 ± 2 and 3141 ± 2 Da, corresponding to the 5′-product with 2′,3′-cyclic phosphate terminus (calculated mass = 3048) and the 3′-product with a free 5′-OH group (calculated mass = 3141), respectively (Figure 6).

Interestingly, in the mass spectrum of the cleavage products of 17DS with Pb^{2+}, a small peak (∼40% of the major peaks) was also observed (mass = 3065 ± 2 Da) in addition to the two major signals that were attributed to the products containing 2′,3′-cyclic phosphate or 5′-OH terminus. This small peak is consistent with the hydrolysis of 2′,3′-cyclic phosphate (calculated mass = 3048), resulting in a 5′ cleavage product bearing a 3′ (or 2′)-monophosphate termi-

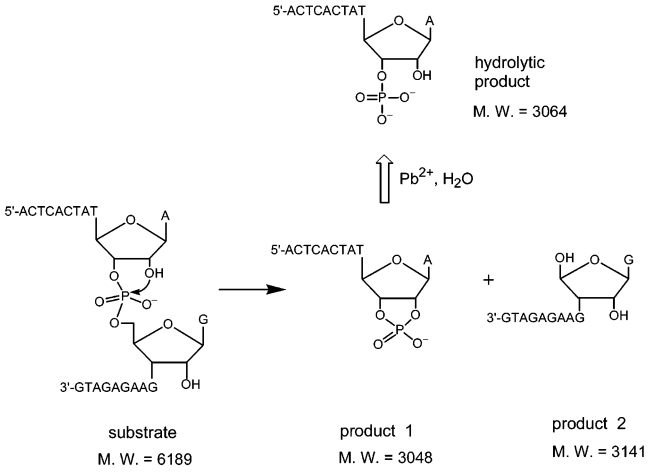

FIGURE 6: Proposed reaction mechanism of substrate cleavage catalyzed by the 17E DNAzyme. The calculated molecular weights (MW) of the substrate and the products are indicated.

nus (calculated mass = 3064) (Figure 6). When the enzyme−substrate reaction time was increased from 15 min to 8 h, the reaction mixture initiated with Mg^{2+} and Zn^{2+} contained mostly cyclic phosphate product. However, the reaction mixture initiated with Pb^{2+}, which contained mostly cyclic phosphate after 15 min of reaction, produced mostly hydrolyzed product after 8 h of reaction. This suggests that Pb^{2+} is able to catalyze a second step that is not catalyzed by Mg^{2+} or Zn^{2+}, as was also observed in the case of the leadzyme (*4*).

To provide further insight into the lead-dependent reaction mechanism, the cyclic phosphate product was purified and added to an excess of enzyme covalently bound to the second product ($17EP_2$) and allowed to react in the presence of Pb^{2+}. Previous ligation studies (*34*) had indicated that there is no ligation of products to reform the substrate after 21 h with various temperatures, salt concentrations, and metal ions at pH 7.4. Therefore, the possibility that the two products ligate and then react with Pb^{2+} to form the hydrolyzed product without forming the cyclic intermediate can be eliminated. With no substrate added to the reaction mixture, the only hydrolyzed product found in the product mixture must have formed via degradation of the cyclic phosphate by Pb^{2+}. For comparison, the cyclic product was also allowed to react in the presence of Pb^{2+} alone and in the presence of $17EP_2$ alone.

The MALDI-MS results (Figure 7) indicate that in the presence of $17EP_2$ alone, there is no hydrolysis of the cyclic phosphate, even after 3 h (results not shown). After 2 min in the presence of Pb^{2+} alone and $17EP_2$ with Pb^{2+}, the product mixtures contain about 10 and 25%, respectively, more cyclic product than hydrolyzed product. However, after 5 min, the product mixture from the reaction with Pb^{2+} alone still contained about 20% more cyclic product, whereas the reaction with both Pb^{2+} and $17EP_2$ produced mostly hydrolyzed product after 5 min. After 15 min of reaction, the sample with both Pb^{2+} and $17EP_2$ produced a spectrum in which the peak corresponding to the cyclic product had almost disappeared into the baseline. The reaction with Pb^{2+} alone produced about 50% more hydrolyzed product than cyclic product after 15 min. These results are comparable to those obtained by Pan and Uhlenbeck with the leadzyme, which found that hydrolysis of the cyclic phosphate occurred about 24-fold slower in the presence of Pb^{2+} alone than with both Pb^{2+} and the leadzyme (*4*).

These results show that the cleavage reaction catalyzed by 17E in the presence of Pb^{2+} occurs in two steps: formation of a 2′,3′-cyclic phosphate and subsequent hydrolysis to form either a 2′- or 3′-phosphate (Figure 6). Because this reaction also occurs in the presence of Pb^{2+} alone, albeit somewhat more slowly, this suggests that hydrolysis of the cyclic phosphate is dependent on Pb^{2+}. The rate of hydrolysis was measured by biochemical assays. With Pb^{2+}, the average rate of hydrolysis measured in four independent assays was approximately 0.114 ± 0.014 min^{-1} with the enzyme/P_2 complex present. In the absence of $17EP_2$, the rate is approximately 2-fold slower (0.060 ± 0.007 min^{-1}). When Mg^{2+} was used, no hydrolysis was observed after 48 h both with and without $17EP_2$ present. The fact that the second step does not occur with other metal ions indicates that Pb^{2+} itself is catalytic. However, the presence of $17EP_2$ speeds up the hydrolysis, indicating that the enzyme is perhaps involved in proper positioning of the Pb^{2+} ion for hydrolysis. Since both the leadzyme and the 17E DNAzyme make use of the same cofactor, and Pb^{2+} itself seems to have catalytic properties for both reactions, it makes sense that both enzymes catalyze the cleavage of substrate through the same two-step mechanism.

DISCUSSION

Three Different in Vitro Selection Experiments Resulted in a Similar 8−17 DNAzyme Motif. Variants of the 8−17 DNAzyme were isolated through in vitro selection by three different groups under three different conditions involving 10 mM Mg^{2+} (*26*), 0.5 mM Mg^{2+}/50 mM histidine (*28*, *29*), or 100 μM Zn^{2+} (*25*) (Table 1). The sequence and proposed secondary structure were defined by Santoro and Joyce (*26*), and the similarity among the DNAzymes obtained from the different selection conditions was noted (*25*, *27*).

The finding that a similar motif was obtained from three independent selections is quite surprising since these three selections not only have different designs of the initial library but also were carried out under different selection conditions, including different cofactors (Table 1). The isolation of the same sequence motif in three distinct and independent in vitro selections can be attributed to at least four factors. First, this structural motif may have unique features, such as appropriately positioned metal binding sites or nucleic acid functional groups, which are especially well-suited for the breaking of the target phosphodiester bond. Second and perhaps more importantly, the small size of the catalytic core (15 nucleotides) allows it to occur at higher frequency than bigger structural motifs within the same random sequence pool. Third, variations for sequences containing 15 nucleotides are more thoroughly represented than those of larger structural motifs. Actually, among these 15 nucleotides, the six bases at the stem of the 3-base-pair hairpin are variable, further increasing the opportunity of selecting this structural motif. Finally, all three selections (for 8−17, 17E, and Mg5) adopted a similar selection strategy: the DNA pool was attached to the solid support and then was eluted off the column upon the cleavage of a ribonucleotide phosphodiester bond within a conserved sequence region.

For the purpose of evaluating the physiological roles of various RNA structures, Bourdeau et al. searched the

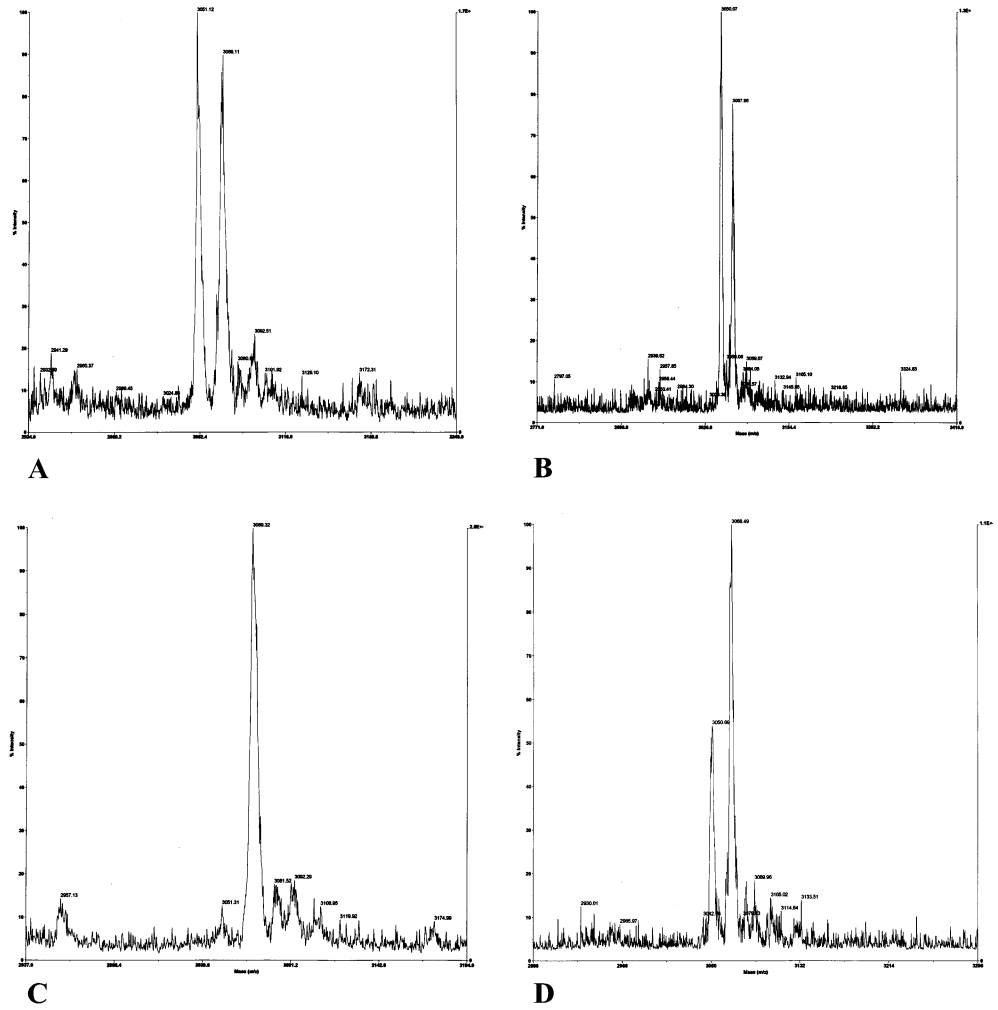

FIGURE 7: Reaction mixtures contained 5 μM 17EP$_2$, 2.5 μM cP$_1$, 200 μM Pb^{2+}, and 50 mM HEPES (pH 7.4). Spectra A and C are from the reaction of the cyclic phosphate product with Pb^{2+} and 17EP$_2$ at 2 min (A) and 15 min (C). Spectra B and D were taken from the reaction of the cyclic phosphate product alone with Pb^{2+} at 2 min (B) and 15 min (D). The hydrolysis of the cyclic phosphate proceeds more quickly in the presence of the enzyme.

sequence database for the distribution of RNA motifs in natural sequences (*35*). They revealed 54 occurrences of RNA motifs having the same sequence as the 8−17 DNAzyme. Such occurring frequency is very low as compared with two other RNA-cleaving nucleic acid enzymes, the hammerhead ribozyme (2788 occurrences) and the leadzyme (2808 occurrences). It was suggested that the low distribution of 8−17 motif was due to its being detrimental to the host organism.

8−17 DNAzyme Is a Lead-Dependent DNAzyme. Previous studies have indicated that the three different variants of the 8−17 DNAzyme are active in the presence of Mg^{2+}, Mn^{2+}, Ca^{2+}, or Zn^{2+} (*25*−*29*). However, the more comprehensive survey of divalent metal ions presented here shows that all three variants of the 8−17 DNAzyme are much more active with Pb^{2+} than with the other divalent metal ions examined (Figure 2 and Table 3). Therefore this 8−17 DNAzyme is a lead-dependent DNAzyme.

The high lead-dependent activity of this 8−17 DNAzyme is surprising because none of the three in vitro selection protocols used to isolate these enzymes involved Pb^{2+} in the selection. This kind of unexpected metal ion selectivity during the in vitro selection process often occurs (*6*), and a negative selection strategy has been shown to suppress the unwanted metal ion dependent activity and thus increase the desired metal ion selectivity (*36*).

Lead hydrate has one of the lowest pK_a's among metal hydrates (Table 1), and under physiological pH, deprotonation of lead hydrate occurs more easily than with other metal hydrates. The deprotonated lead hydroxide makes it possible to remove the proton from the 2′-hydroxyl of ribo-A at the putative cleavage site, just like in the lead−tRNA^{phe} complex (*3*, *8*). However, the pK_a of lead hydrate explains only partially its high lead-dependent activity. As shown in Table 2 and Figure 2, the metal-dependent activity only follows the pK_a in a rough order, and deviation from the correlation occurs. For example, the enzyme exhibits low activity with Ni^{2+} even though its hydrate has a relatively low pK_a (9.86). Moreover, the hammerhead RNAzyme is not active with Pb^{2+} (*37*), and no Pb^{2+}-dependent activity of the 10−23 DNAzyme has been reported. Therefore, a specific binding site must be present in order for Pb^{2+} to carry out its function. Indeed, metal-binding curves of the 17E DNAzyme (Figure 3) indicated that the enzyme binds Pb^{2+} tighter than other divalent metal ions with an apparent K_d in the order of $Pb^{2+} > Zn^{2+} > Mg^{2+}$.

This 8−17 DNAzyme Is a Highly Efficient DNAzyme. Because of the findings that this 8−17 DNAzyme shows

lead-dependent activity, we carried out a detailed kinetic study of its lead-dependent activity and put the results in the perspective of lead-tRNA^{phe} and the leadzyme, a lead-dependent RNAzyme.

From Figure 3, the apparent maximum rate of the DNAzyme was determined to be ~7 min^{-1} at pH 6.0. Since the slope of the pH dependence curve is ~1 (Figure 4), the apparent maximum rate of the enzyme at physiological pH (7.5) can be estimated to be ~220 min^{-1}, which is among the highest in DNA/RNAzymes and is much faster than the ~1 min^{-1} observed for the leadzyme (*4*, *10*).

Previous studies have shown that, for the leadzyme, changing the ribonucleobases at several positions to either deoxyribonucleobases or other modified bases resulted in significant decreases in either the substrate binding and/or cleavage (*13*, *15*, *17*). For this 8−17 DNAzyme, with the exception of the scissile ribonucleobase, all other nucleotides are DNA. The enzyme is effective in cleaving all four bases at the scissile ribonucleobase positions, with about 10-fold preference for purine bases (Table 4). Further sequence variation studies indicate that the G$^{1.1}$•T$^{2.1}$ wobble pair is essential for the DNAzyme's activity, as reversing the wobble pair or changing the wobble pair to a G−C pair abolishes its activity. These results could indicate that the wobble pair is necessary for correctly binding the metal ion. In addition, introduction of a second wobble pair either on the 3′ or the 5′-side of the G$^{1.1}$•T$^{2.1}$ wobble pair caused the reaction rate to decrease 10- and 2-fold, respectively, in the presence of Pb^{2+} (Table 3). This decrease in reaction rate is most likely because of destabilization of the enzyme−substrate complex.

Further sequence variations in the conserved loops (A^{6}G^{7}C^8 and T^{12}C^{13}G^{14}A^{15}A$^{15.0}$) and the canonical core stem between the two loops indicate that the conserved core shown in Figure 1D is required for the DNAzyme activity. For example, switching the A^{6}G^{7}C^8 loop to C^{6}G^{7}A^8 or adding an A to the loop (i.e., A$^{6.0}$A^{6}G^{7}C^8) resulted in a dramatic decrease in the Pb^{2+}- and Zn^{2+}-dependent activity. In addition, while changing the C^4−G^{10} pair in the canonical core stem to A^4−T^{10} caused only minimal changes in enzyme activity (which is consistent with previous findings (*26*, *27*)), adding a new G−C pair to the stem decreased the enzyme activity by more than 2 orders of magnitude. Finally, similarly to the results found in the Mg^{2+}- (*26*) and Ca^{2+}-dependent (*27*) activity studies, deletion of A$^{15.0}$ can be tolerated while deletion of T^{12} cannot for Pb^{2+}- or Zn^{2+}-dependent activity (Table 3).

In general, results obtained in this study, combined with those reported for Mg^{2+}- (*26*) and Ca^{2+}-dependent (*27*) activity studies for 8−17 DNAzymes indicate that sequence variations seem to affect Mg^{2+}-, Ca^{2+}-, Pb^{2+}-, or Zn^{2+}-dependent activities in a similar manner, suggesting that the sequence specificity is independent of the catalytic metal ions used in the reaction. This is despite that the apparent binding affinity of the metal ions are quite different and that Pb^{2+} catalyzes the reaction using a different mechanism from those used by other metal ions (see next section).

This 8−17 DNAzyme Is a DNAzyme with a Two-Step Mechanism. Product analysis by MALDI-MS demonstrated that Mg^{2+}, Zn^{2+}, and Pb^{2+} all catalyze the cleavage reaction of this 8−17 DNAzyme by the formation of a product containing 2′,3′-cyclic phosphate. This cleavage pattern is similar to those catalyzed by the hammerhead (*38*), the hairpin (*39*), the Neurospora (*40*), and the HDV ribozymes (*41*), as well as to the 10−23 DNAzyme (*26*). The formation of the 2′,3′-cyclic phosphate during cleavage is consistent with an internal transesterification mechanism, in which the 2′-OH group at the cleavage site undergoes in-line attack on the scissile phosphorus, forming a pentacoordinated phosphate intermediate followed by the leaving of the 5′-oxygen (Figure 6) (*42*, *43*).

In addition to the above transesterification step, Pb^{2+} catalyzes a second step of further hydrolysis of the 2′,3′-cyclic phosphate (Figure 6), as shown by the product analysis (Figure 7). The second hydrolysis step was not observed in Mg^{2+}- or Zn^{2+}-catalyzed reactions for the same DNAzyme, even though their activities vary with pH and sequences in a similar fashion as with Pb^{2+} (*25*). Similar hydrolysis products have also been observed by Pan and Uhlenbeck in the leadzyme, an RNAzyme (*4*). They indicated that the hydrolysis product may result from a second step, further hydrolysis of the 2′,3′-cyclic phosphate, or from a separate pathway independent of the 2′,3′-cyclic phosphate. To prove that the 2′,3′-cyclic phosphate is an intermediate in the Pb^{2+}-catalyzed reaction, we have isolated the product containing the 2′,3′-cyclic phosphate through a Mg^{2+}-dependent reaction. Reaction of the isolated product with other components of the 17E DNAzyme in the presence of Pb^{2+} resulted in the expected hydrolysis product (Figure 7). Furthermore, since ligation studies (*34*) had indicated that there is no ligation of products to reform the substrate after 21 h with various temperatures, salt concentrations, and metal ions at pH 7.4, the possibility that the two products ligate and then react with Pb^{2+} to form the hydrolyzed product without forming the 2′,3′-cyclic phosphate intermediate can be eliminated.

This two-step mechanism has been observed in protein ribonucleases and in the leadzyme RNAzyme (*4*). We have now demonstrated for the first time that a DNAzyme such as this 8−17 DNAzyme may use the same two-step mechanism; thus, the mechanism is no longer unique to protein enzymes and ribozymes. Since Pb^{2+} is involved in the two-step mechanisms of both the leadzyme and the 17E DNAzyme, it is tempting to conclude that the two-step mechanism is a property of all Pb^{2+}-dependent cleavage reactions. However, as pointed out by Pan and Uhlenbeck (*4*), this conclusion is not correct, as no evidence of catalytic hydrolysis of the 2′,3′-cyclic phosphate was found in the Pb^{2+} cleavage product of yeast tRNA^{phe}. Therefore, a specific, three-dimensional structure may be required to form a Pb^{2+}-binding site to complete this two-step mechanism. This 8−17 DNAzyme provides a simple, stable, and cost-effective model system for the elucidation of Pb^{2+}-binding sites in nucleic acid enzymes and their roles in catalyzing the two-step mechanism.

ACKNOWLEDGMENT

We wish to thank Prof. Tao Pan for advice on enzyme assays.

REFERENCES

1. Westhof, E., and Hermann, T. (1999) *Nat. Struct. Biol. 6*, 208−209.
2. Scott, W. G. (1999) *Curr. Opin. Chem. Biol. 3*, 705−709.

3. Brown, R. S., Hingerty, B. E., Dewan, J. C., and Klug, A. (1983) *Nature* (*London*) *303*, 543−6.
4. Pan, T., and Uhlenbeck, O. C. (1992) *Nature 358*, 560−563.
5. Li, J., and Lu, Y. (2000) *J. Am. Chem. Soc. 122*, 10466−10467.
6. Lu, Y. (2002) *Chem. Eur. J. 8*, 4588−4596.
7. Werner, C., Krebs, B., Keith, G., and Dirheimer, G. (1976) *Biochim. Biophys. Acta 432*, 161−175.
8. Brown, R. S., Dewan, J. C., and Klug, A. (1985) *Biochemistry 24*, 4785−4801.
9. Pan, T., and Uhlenbeck, O. C. (1992) *Biochemistry 31*, 3887−3895.
10. Pan, T., Dichtl, B., and Uhlenbeck, O. C. (1994) *Biochemistry 33*, 9561−9565.
11. Sugimoto, N., and Ohmichi, T. (1996) *FEBS Lett. 393*, 97−100.
12. Ohmichi, T., and Sugimoto, N. (1997) *Biochemistry 36*, 3514−3521.
13. Ohmichi, T., and Sugimoto, N. (1997) *Bull. Chem. Soc. Jpn. 70*, 2743−2747.
14. Kim, M. H., Katahira, M., Sugiyama, T., and Uesugi, S. (1997) *J. Biochem.* (*Tokyo*) *122*, 1062−1067.
15. Chartrand, P., Usman, N., and Cedergren, R. (1997) *Biochemistry 36*, 3145−3150.
16. Katahira, M., Kim, M. H., Sugiyama, T., Nishimura, Y., and Uesugi, S. (1998) *Eur. J. Biochem. 255*, 727−733.
17. Ohmichi, T., Okumoto, Y., and Sugimoto, N. (1998) *Nucleic Acids Res. 26*, 5655−5661.
18. Legault, P., and Pardi, A. (1997) *J. Am. Chem. Soc. 119*, 6621−6628.
19. Legault, P., Hoogstraten, C. G., Metlitzky, E., and Pardi, A. (1998) *J. Mol. Biol. 284*, 325−335.
20. Hoogstraten, C. G., Legault, P., and Pardi, A. (1998) *J. Mol. Biol. 284*, 337−350.
21. Hoogstraten, C. G., Wank, J. R., and Pardi, A. (2000) *Biochemistry 39*, 9951−9958.
22. Wedekind, J. E., and McKay, D. B. (1999) *Nat. Struct. Biol. 6*, 261−268.
23. Breaker, R. R., and Joyce, G. F. (1994) *Chem. Biol. 1*, 223−229.
24. Geyer, C. R., and Sen, D. (1998) *J. Mol. Biol. 275*, 483−489.
25. Li, J., Zheng, W., Kwon, A. H., and Lu, Y. (2000) *Nucleic Acids Res. 28*, 481−488.
26. Santoro, S. W., and Joyce, G. F. (1997) *Proc. Natl. Acad. Sci. U.S.A. 94*, 4262−4266.
27. Peracchi, A. (2000) *J. Biol. Chem. 275*, 11693−11697.
28. Faulhammer, D., and Famulok, M. (1996) *Angew. Chem., Int. Ed. Engl. 35*, 2837−2841.
29. Faulhammer, D., and Famulok, M. (1997) *J. Mol. Biol. 269*, 188−202.
30. Stage-Zimmermann, T. K., and Uhlenbeck, O. C. (1998) *RNA 4*, 875−889.
31. Dahm, S. C., Derrick, W. B., and Uhlenbeck, O. C. (1993) *Biochemistry 32*, 13040−13045.
32. Santoro, S. W., and Joyce, G. F. (1998) *Biochemistry 37*, 13330−13342.
33. Li, J. Ph.D. Dissertation, University of Illinois at Urbana-Champaign, Urbana, IL, 2000.
34. Pavot, C. M.-B. Master's Thesis, University of Illinois at Urbana-Champaign, Urbana, IL, 2001.
35. Bourdeau, V., Ferbeyre, G., Pageau, M., Paquin, B., and Cedergren, R. (1999) *Nucleic Acids Res. 27*, 4457−4467.
36. Bruesehoff Peter, J., Li, J., Augustine, I. A. J., and Lu, Y. (2002) *Comb. Chem. High Throughput Screening 5*, 327−35.
37. Dahm, S. C., and Uhlenbeck, O. C. (1991) *Biochemistry 30*, 9464−9469.
38. Uhlenbeck, O. C. (1987) *Nature 328*, 596−600.
39. Hampel, A., and Tritz, R. (1989) *Biochemistry 28*, 4929−4933.
40. Saville, B. J., and Collins, R. A. (1990) *Cell 61*, 685−696.
41. Thill, G., Vasseur, M., and Tanner, N. K. (1993) *Biochemistry 32*, 4254−4262.
42. Zhou, D.-M., and Taira, K. (1998) *Chem. Rev. 98*, 991−1026.
43. Kuimelis, R. G., and McLaughlin, L. W. (1998) *Chem. Rev. 98*, 1027−1044.
44. Richens, D. T. (1997) *The Chemistry of Aqua Ions*, John Wiley and Sons, New York.
45. Hertel, K. J., Pardi, A., Uhlenbeck, O. C., Koizumi, M., Ohtsuka, E., Uesugi, S., Cedergren, R., Eckstein, F., Gerlach, W. L., Hodgson, R., and Symons, R. H. (1992) *Nucleic Acids Res. 20*, 3252.

BI027332W